CSIRO PUBLISHING

Aust. J. Chem. **2015**, *68*, 1918–1925
http://dx.doi.org/10.1071/CH15102

Full Paper

The Cooperative Effect in Dendronized Chitosan Microbeads

Ana Agustina Aldana,[A] *Miriam C. Strumia,*[A] *and Marisa Martinelli*[A,B]

[A]Instituto Multidisciplinario de Biología Vegetal (IMBIV), CONICET, Departamento de Química Orgánica, Facultad de Ciencias Químicas, Universidad Nacional de Córdoba, Haya de la Torre y Medina Allende, X5000HUA, Córdoba, Argentina.
[B]Corresponding author. Email: mmartinelli@fcq.unc.edu.ar

The present study evaluates the cooperative effects of dendronized chitosan microbeads with tris- and hexa-functionalized dendrons for capturing copper and for further use as catalysts. The dendronized microbeads were characterized by infrared spectroscopy, scanning electron microscopy, thermogravimetry, swelling capacity analysis, and atomic absorption spectroscopy. A correlation between the number and type of functional groups at the dendritic surface of the dendronized microbeads and the retention of copper highlights structural features of the cooperative effect. It is demonstrated that covalently bound dendrons can modulate the properties of chitosan, which has shown potential as a catalyst for the development of a novel materials.

Manuscript received: 4 March 2015.
Manuscript accepted: 14 May 2015.
Published online: 16 June 2015.

Introduction

Modifying the surface of seemingly inert polymers to obtain functional materials has posed one of the greatest challenges in chemical research in recent years. Advances in the chemical design of such polymers are an important step towards forming novel multifunctional materials with new physicochemical properties, thus widening the spectrum of their application in different areas of technologies.[1,2] The modifying agent needs to be able to maintain an effective link with the surface so that if the network is involved in serial reactions, the original polymeric structure remains unaltered throughout the entire process. Because of the increased demand for novel macromolecules, researchers have centred their attention to highly branched dendritic structures. These molecules are ideal platforms for studying cooperative effects due to the uniform functional groups at their peripheries.[3] Dendrimers draw particular interest across disciplines as a result of their well-defined structures, shapes, and sizes when compared with other types of polymers. Dendritic structures are mainly characterized by their multivalency, a consequence of the large number of surface end groups within the same molecule, thus enabling them to interact with several chemical entities and thus generate hierarchical complexes with high binding affinities.[4]

Regularly branched dendrons can be attached to a focal point, linear polymers, or a surface, thus giving rise to dendronized polymers and dendronized surfaces.[5] For instance, a significantly positive dendritic effect was observed in the antibody binding capacity of immobilized bovine serum albumin coupled to a dendronized support.[6] In addition, our research group recently reported the case of a dendron as a mediator in the electrocatalysis of nicotinamide adenine dinucleotide oxidation onto carbon electrodes. The electrochemical properties were directly related to the number of electroactive functional groups incorporated into the dendritic molecule.[7]

Biopolymers are biocompatible, biodegradable, and non-toxic, and have adsorption properties, film forming ability, bio-adhesion properties. In some cases, biopolymers are of cationic or anionic nature, and most of them are hydrophilic. Chitosan[8] in particular is a biopolymer produced by the alkaline N-deacetylation of chitin, widely found in the exoskeletons of shellfish and crustaceans. The growing need for new sources of low-cost adsorbent, increasing global problems of waste disposal, and rising cost of synthetic resins undoubtedly make chitosan an attractive material. It has been used in a wide range of applications in different fields.[9–11] The interest in using renewable resources in complex molecular architectures has arisen as a consequence of the quest to find substitutes for oil-based raw materials.[12,13] However, polysaccharides, such as chitosan or cellulose, suffer from a few disadvantages and require further development to achieve the targeted results and desired range of efficiency.[14,15] To overcome some of the disadvantages of natural polymers, different strategies have been developed.[16–19]

One of our previous works focussed on the functionalization of chitosan for use in different fields of application. For instance, we have developed dendronized chitosan-based films with ideal properties for wound dressings, enabling them to maintain a moist environment at the wound interface and act as a barrier to microorganisms, thus removing excess exudates.[20] These films featured the known advantages of chitosan such as biocompatibility, biodegradability, antimicrobial, and antifungal properties.

The present work aims at exploring the cooperative dendritic effect on chitosan functionalization. To this end, we prepared

Journal compilation © CSIRO 2015

chitosan microbeads with the aim of improving the mechanical properties of chitosan, consequently yielding a material with water dispersibility and high surface-to-volume ratio. The microbeads were functionalized with dendrons to create a dendritic surface exhibiting a highly defined three-dimensional architecture and known behaviours as a consequence of the specifically modified surfaces. These dendronized microbeads were used as a chelating agent for copper ion, Cu^{2+}, and were further tested as a heterogeneous catalyst support. The dendritic molecules provide a unique macromolecular environment for the coordinated metal, influencing the regio- and chemoselectivity of catalytic reactions. To the best of our knowledge, this is the first report using dendronized biopolymers as a catalyst support.

Results and Discussion

Synthesis of Dendronized Microbeads

Due to their high surface-to-volume ratio, chitosan microbeads are ideal candidates for conducting surface dendronization and analysis of cooperative effects. With this in mind, the coacervation precipitation method[21] was used to prepare chitosan microbeads with a diameters ranging between 0.8 and 1.2 mm and a low dispersity, as demonstrated by scanning electron microscopy (SEM) (Fig. 1a). The surface functional groups of chitosan were activated with epoxy groups for further linkage to the amine-bearing dendrons using epichlorohydrin (ECH) or butylene diglycidyl ether (BDGE) (Fig. 2 and Fig. S1, Supplementary Material) to analyze the effect of chain length on the subsequent binding of dendrons. ECH or BDGE was used as spacer linkers and cross-linking agents to facilitate the subsequent covalent bond formation of the dendron and to enhance the stability of the microbeads, thus improving their mechanical properties.

The Fourier transform infrared (FT-IR) spectra of the activated chitosan (Ch) microbeads confirmed the surface functionalization (Fig. 3). ECH-activated Ch microbeads (Ch-ECH) revealed a new signal at 3027 cm^{-1} corresponding to C–H stretching vibration of the epoxy group; the stretching vibration of C–O–C appears at 1033, 1249, and 827 cm^{-1}. The C–H stretching, corresponding to the epoxy group of the BDGE, in spectrum of Ch-BDGE appears at 3035 cm^{-1}, and the bands assigned to the asymmetrical and symmetrical stretching vibration C–O–C of the ether group appear at 1240 and 824 cm^{-1}, respectively. In both cases, the typical absorptions of chitosan were also present.[22] The morphology of the microbeads was not affected by the activation process, as evidenced by SEM analysis (Fig. 1b).

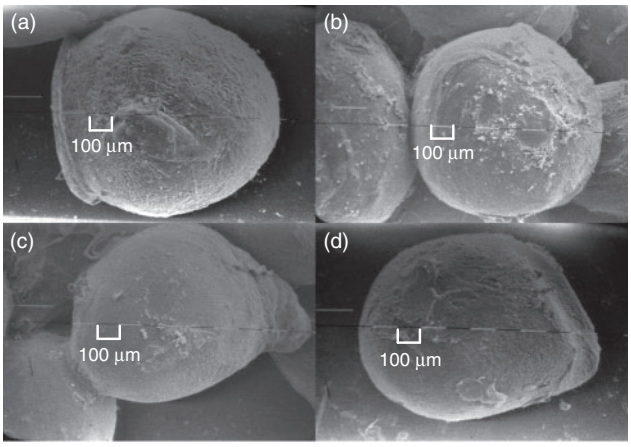

Fig. 1. Scanning electron microscopy images (zoom 4×80) of (a) chitosan (Ch), (b) Ch-ECH, (c) Ch-ECH-BA, and (d) Ch-ECH-BB.

For the dendronization of the epoxy-bearing microbeads, dendrons BA (Behera's amine, tris[(*tert*-butoxycarbonyl)ethyl] aminomethane) and BB (bis Behera's amine, *N*,*N*′-bis[tris((*tert*-butoxycarbonyl)ethyl)methyl]-5-aminephthalamide) were linked through the amine group of the dendron focal point yielding Ch-ECH-BA, Ch-ECH-BB, Ch-BDGE-BA, and Ch-BDGE-BB, respectively (Fig. 2 and Figs. S1 and S2, Supplementary Material). BA and BB dendrons were selected because of their biocompatible properties,[23] and well-known nucleophile properties for opening epoxide groups. Table 1 shows the percentage incorporation of dendrons into each microbead. The amount of dendron was quantitatively determined by titration of the free epoxy group before and after dendronization.

Dendronization of the surface groups of the microbeads was clearly evidenced by diffuse reflectance IR spectroscopy. The spectra of the dendronized products showed a typical band at 1724 cm^{-1} corresponding to C=O stretching and bands at 850 and 760 cm^{-1} corresponding to C–O–C stretching of the ester and *tert*-butylic groups of dendron, respectively, confirming the presence of BA and BB (Fig. 3). Other changes in the spectra were not observed in the dendronized sample due to the high intensity of the absorption bands of chitosan.

According to the titrations, the amount of BA dendron incorporated was higher than that of BB dendron, probably due to the presence of a higher number of *tert*-butyl groups on the periphery, generating greater steric hindrance. In addition, the aromatic amine reactivity of BB dendron was lower than that of the aliphatic amine of BA dendron.[24] BDGE proved to be a more effective linker, possibly because its longer chain length decreases the effects of steric hindrance. The SEM results show that the morphology and size of the microbeads were retained after dendronization (Fig. 1c, d).

Thermogravimetry analysis (TGA) and differential scanning calorimetry (DSC) were used to analyze the thermal stability of the chitosan microbeads and dendronized products. Thermal stability is an important feature when it comes to applications limited by low thermal and mechanical stability of chitosan. The behavioural pattern was similar for the different matrices (i.e. Ch-ECH, Ch-ECH-BA and Ch-BDGE, Ch-BDGE-BA). The thermogravimetric profiles reveal two stages of mass loss. The first degradation stage at around 100–150°C, with a mass loss of 2–10 %, is related mainly to the loss of water physically adsorbed onto the surface of the materials. Ch undergoes a mass loss of 50 % at 298°C.[25] The second degradation stage of Ch-ECH and Ch-ECH-BA was observed at 264°C and 296°C, respectively, with a mass loss of ~40 %. These values represent the temperatures of maximum mass loss in the polymeric materials and were established from the first-derivative thermogravimetric plots. The temperature of the second degradation stage of Ch-ECH-BA is higher than that of Ch-ECH, indicating that the new matrix is thermally more stable than the non-dendronized microbeads. The DSC profiles for Ch-ECH and Ch-ECH-BA show three exothermic peaks at 256.6, 266.7, and 279.0°C, and 277.4, 288.9, and 300.6°C, respectively.[26] These exothermic peaks can be attributed to the thermal degradation of the materials. The significant difference observed in the position of the exothermic peaks of Ch-ECH and Ch-ECH-BA indicates surface modification of the microbeads.[27]

Moreover, the TGA profiles of the modified chitosan matrix (Ch-ECH-BA) and the physical mixture of chitosan and BA

provide evidence of chemical bonding between the components of the beads. The characterization results confirm that the formation of the new dendronized materials occurred successfully and increased both surface functionalization and thermal stability.

Hydrolysis of Ester Groups on the Periphery

In order to increase the hydrophilicity of the microbead surface and modify the affinity towards different ligands, the ester groups on the periphery of the dendrons were partially hydrolyzed to acid groups. An acid-mediated cleavage was successfully performed to yield carboxylic groups at the surface (Fig. S1, Supplementary Material). The degree of hydrolysis was determined by potentiometric titration (Table 1). The diffuse-reflectance IR spectra of the hydrolyzed matrices revealed a shift in the signal from 1726 cm^{-1}, corresponding to C=O stretching of the ester dendron group, to 1714 cm^{-1}, corresponding to the carboxylic group. The diffuse-reflectance IR spectra of the hydrolyzed matrices revealed a new band at 1714 cm^{-1} corresponding to C=O stretching of the carboxylic group. The intensity of the signal corresponding to C=O stretching of the ester dendron group decreases.

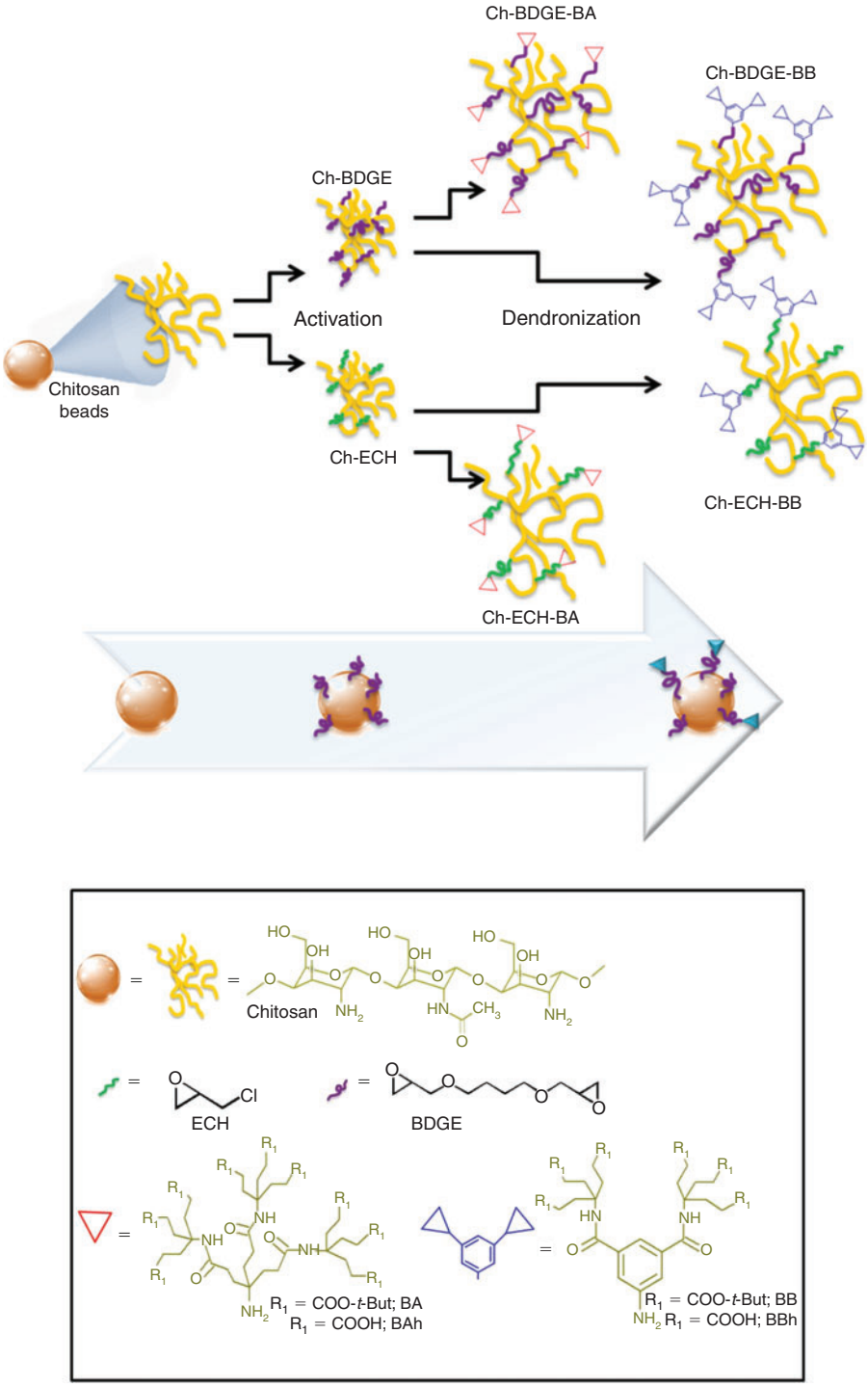

Fig. 2. Schematic representation of the synthetic routes used for the preparation of the dendronized chitosan microbeads.

A higher percentage of hydrolysis was obtained for the reaction of the Ch-ECH-dendron matrices than that for Ch-BDGE-dendron. This could be explained by a combination of the degree of cross-linking and the hydrophilicity imparted by the BDGE linker to the chitosan microbead, thus hindering the hydrolysis reaction. The highest percentage of hydrolysis was observed for Ch-ECH-BB, attaining a 97.4 % reaction yield.

Swelling Studies

The stability of chitosan matrices is particularly significant for reliable, cost-effective, and reproducible applications. Thus, studying the swelling behaviour of the microbeads at different pH values is important. Swelling studies were performed at pH values of 1.2 and 7.4, representing the conditions above and below the pK_a of the amine groups of chitosan, in order to evaluate the behaviour of the network carrying either positively charged ammonium groups ($-NH_3^+$) or neutral amine groups ($-NH_2$).[28]

The results in Fig. 4 show the variations in behaviours of the dendronized and non-dendronized systems at two different pH values.

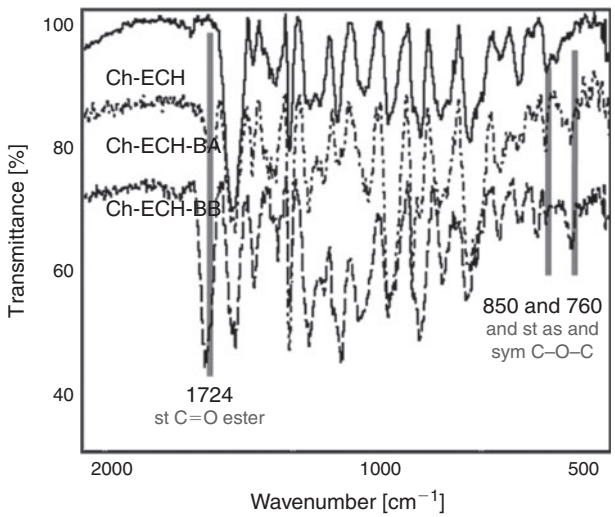

Fig. 3. FT-IR spectra of the chitosan microbeads Ch-ECH, Ch-ECH-BA, and Ch-ECH-BB.

In general, swelling indexes of Ch-BDGE-dendron were lower than those of Ch-ECH-dendron. The former showed similar swelling values at both pHs, possibly owing to the bifunctionality and longer chain length of BDGE, which would also act as a cross-linking agent. Moreover, the swelling indexes of Ch-BDGE-dendron were similar for matrices bearing either *tert*-butyl or COOH groups on the surface. This suggests that the swelling of Ch-BDGE-dendron matrices was driven by the free functional groups of the chitosan chain.

As expected, a higher hydrophilic character was evidenced in the swelling value of Ch-ECH-BAh (hydrolyzed Ch-ECH-BA microbeads) when compared with that of Ch-ECH-BA at pHs 1.2 and 7.4. Intriguingly, Ch-ECH-BB showed a higher swelling value than Ch-ECH-BBh (hydrolyzed Ch-ECH-BB microbeads) at pH 1.2. This may be caused by the close proximity of the acid groups on the periphery that are capable of forming hydrogen bonds, thereby hindering the entry of water into the network.

For Ch-ECH-BAh and Ch-ECH-BBh microbeads, the swelling values increased at pH 7.4 when compared with the non-hydrolyzed microbeads, likely as a result of repulsive interactions among the acid groups on the periphery that are ionized at that pH.

The difference in the swelling values of the hydrolyzed and non-hydrolyzed microbeads was greater between Ch-ECH-BBh and Ch-ECH-BB, in agreement with the high degree of hydrolysis (Table 1). At pH 7.4, Ch-ECH-BAh and Ch-ECH-BBh matrices showed similar swelling indexes. The effect of the lower degree of dendronization and the higher amount of peripheral groups for Ch-ECH-BB is thus compensated (Table 1).

In summary, the number and type of functional groups on the periphery are the major determinants of the swelling indexes. Thus, dendronization has a structural, rather than geometrical, effect on the swelling properties of the chitosan microbeads. It is worth mentioning that a larger number of COOH groups at the surface do not correlate with a higher swelling index in acid medium, which highlights the formation of intramolecular hydrogen bridges. Similar results were reported by Rupp et al., who demonstrated the influence of polyamidoamine dendrimers on surface-modified silicone. Different terminal groups (NH_2 or COOH) pertaining to the original surface seem to influence the conditioning process and impact on wettability.[29]

Table 1. Coupling of Behera's amine (BA) and bis Behera's amine (BB) dendrons on Ch-ECH and Ch-BDGE microbeads and hydrolysis of functional periphery groups (ester to acid)

Matrix	Epoxy groups[A] [$\times 10^{-4}$ mol g^{-1} matrix]	Dendron [$\times 10^{-4}$ mol g^{-1} matrix]	Dendronization yield[B] [%]	Hydrolysis of ester groups [%]	Acid groups [$\times 10^{-4}$ mol g^{-1} matrix]
Ch-ECH	1.80	–	–	–	
Ch-ECH-BA	0.72	1.08	100	–	
Ch-ECH-BAh	0.72	1.08	–	45.7	1.48
Ch-ECH-BB	1.53	0.27	25	–	
Ch-ECH-BBh	1.53	0.27	–	97.4	1.58
Ch-BDGE	3.78	–	–	–	
Ch-BDGE-BA	1.51	2.27	100	–	
Ch-BDGE-BAh	1.51	2.27	–	18.9	1.29
Ch-BDGE-BB	2.98	0.80	35		
Ch-BDGE-BBh	2.98	0.80	–	60.4	2.90

[A]Epoxy groups on matrix that are free after dendronization.
[B]According to dendron/epoxy groups mol ratio of 1 : 0.6.

Copper Retention

It is known that copper ions immobilized on polymer matrices can potentially bind proteins, catalyze oxidation reactions, or purify polluted water.[30–32] We therefore analyzed the copper absorption capability of the dendronized chitosan microbeads. The relevance of the degree of dendronization and the balance between the nature of each of the peripheral functional groups were studied.

As shown in Table 2, copper retention after incubation of the matrices with copper nitrate was higher for the dendronized microbeads compared with that obtained with Ch, Ch-ECH, and Ch-BDGE. The retention capacity of Ch-ECH and Ch-BDGE microbeads were lower than the capacity of Ch microbeads. Probably, a possible cross-linking with ECH and BDGE decreases copper retention. In contrast, a higher level of copper(II) retention was attained over the dendronized matrix with BB even though the degree of dendronization was lower. This phenomenon could be ascribed to the dendrimer's unique feature of a cooperative surface reflected by the amplified amount of surface functionalities per unit of surface area.[33] For a better analysis of this phenomenon and in order to illustrate the cooperative effect per dendron unit independently of the degree of dendronization, the copper loaded values were normalized using the following equation.

$$\mathrm{Cu}^{n}_{\mathrm{ads}} = (\mathrm{Cu}_{\mathrm{ds}} - \mathrm{Cu}_{\mathrm{s}})\frac{2.27 \times 10^{-4}}{d_{\mathrm{ds}}}$$

where, $\mathrm{Cu}^{n}_{\mathrm{ads}}$ represents the normalized copper loaded values; $\mathrm{Cu}_{\mathrm{ds}}$ and Cu_{s} represent the values of copper loaded on the dendronized beads and non-dendronized beads, respectively; d_{ds} is the number of moles of dendron in 1 g of matrix for dendronized beads, and 2.27×10^{-4} is the maximum number of moles of dendron in 1 g of matrix.

Comparison between the normalized loaded Cu values shows a greater cooperative effect for the matrices modified with BB. The matrices modified with BDGE clearly show the highest value for Ch-BDGE-BAh, whereas the matrices modified with ECH show the highest normalized loaded Cu for Ch-ECH-BB. A lower normalized loaded Cu was observed for Ch-ECH-BBh relative to that of Ch-ECH-BB that correlates with the higher hydrogen binding capacity as previously discussed.

The interaction between Cu^{2+} and the sorbent was confirmed by diffuse-reflectance FTIR spectroscopy and ^{1}H-NMR (Fig. S4, Supplementary Material). The intensity of the band at 1724 cm^{-1} (C=O stretching of peripheral groups of dendron) decreased, appearing at a lower frequency. The major modification derives from coordination with Cu^{2+} Accordingly, the loss in intensity of the band at 2973 cm^{-1} is caused by the change in environment of CH_3 (peripheral ester groups of dendron) after the sorption process. In contrast, there is no significant alteration in the broad band at ~3300–3570 cm^{-1}, associated with −OH and −NH stretching vibrations corresponding to functional groups of chitosan. This could be attributed to a weak interaction between the −OH and −NH functional groups and metal ions.[34]

The dendron–metal interaction was analyzed by comparing the dendron and dendron–copper ^{1}H-NMR spectra. The BA+Cu spectrum (Fig. S4b (spectrum 2), Supplementary Material) shows a noticeable widening of the dendron signals ($-CH_2-CH_2-$, $-CH_2-CH_2-$, and $-C(CH_3)_3$) when compared with BA spectrum (Fig. S4b (spectrum 1), Supplementary Material). In addition, a slight shift of these peaks to upper frequencies was observed (1.54 to 1.56, 1.90 to 2.00, and 2.45 to 2.46, respectively). These results indicate the occurrence of conformational

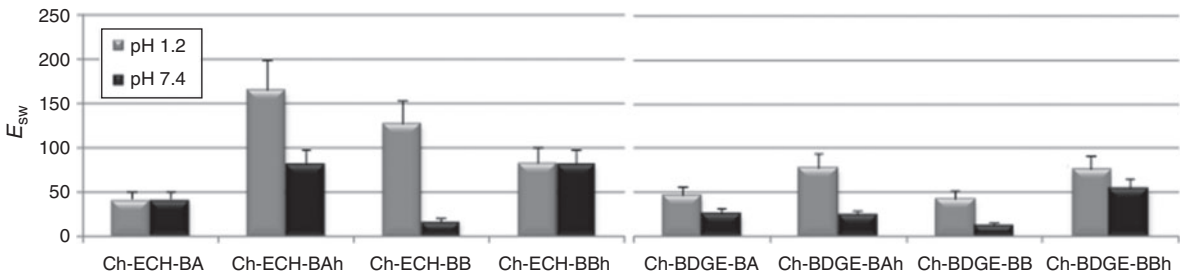

Fig. 4. Swelling index of the modified chitosan microbeads at pHs 1.2 and 7.4.

Table 2. Copper ion adsorption and recovery values on dendronized microbeads

Matrix	Cu loaded [mg g^{-1} matrix]	Normalized loaded Cu [mg g^{-1} matrix]	Cu recovered [%]
Ch	23.6 ± 0.9	–	≈ 100
Ch-ECH	10.4 ± 0.5	–	≈ 100
Ch-ECH-BA	50.4 ± 0.5	84	23.59
Ch-ECH-BAh	62.4 ± 0.7	109	24.06
Ch-ECH-BB	62.3 ± 0.6	436	24.15
Ch-ECH-BBh	51.7 ± 0.6	347	18.80
Ch-BDGE	8.3 ± 0.6	–	≈ 100
Ch-BDGE-BA	47.9 ± 0.4	40	18.93
Ch-BDGE-BAh	50.7 ± 0.5	42	11.69
Ch-BDGE-BB	63.0 ± 0.6	155	19.27
Ch-BDGE-BBh	95.7 ± 0.9	248	11.06

changes in the environment of the proton as a consequence of interaction with the metal, affecting the H shifts, thus resulting in different behaviours between the BA+Cu and free dendron signals.

The stability of the matrix–metal complex was confirmed by washing the copper-loaded microbeads with acid solutions. Table 2 shows a lower copper recovery for Ch-BDGE-dendron, confirming the higher copper binding capacity of the dendronized microbeads when compared with that of the chitosan beads.

It is worth mentioning that the unmodified chitosan microbeads display higher absorption capacities. However, as demonstrated by the washing experiment, the stability of such complexes was rather low, thus limiting the further use of unmodified microbeads. It is therefore clear that the copper binding process is assisted by dendron branches via encapsulation or complexation effects.

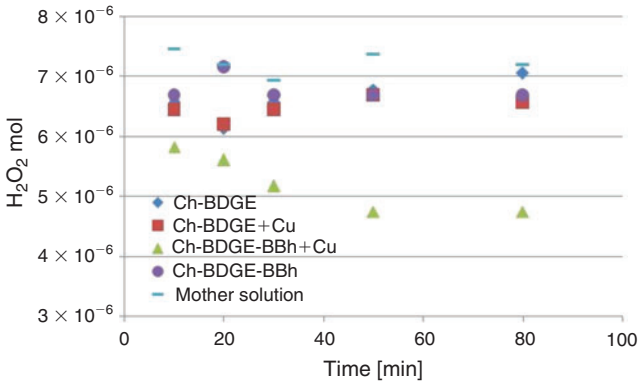

Fig. 5. Reaction of hydrogen peroxide decomposition catalyzed by modified chitosan microbeads.

Testing Dendron and Cu Activity in Hydrogen Peroxide Catalysis

The catalytic decomposition of H_2O_2 has been extensively studied due to its vast applicability in water treatment technologies. Various organic water and soil pollutants can be successfully oxidized and degraded by hydrogen peroxide promoted by iron oxides.[32,35,36] The kinetics of hydrogen peroxide decomposition depends mainly on experimental conditions such as pH, concentration of hydrogen peroxide, and the catalyst. In the case of heterogeneous catalysis, the structure and surface properties of the catalyst have to be taken into account. It is the crystallinity of the particles, rather than their surface area, that largely determines catalytic efficiency.[36]

As a first attempt to explore the potential of copper-loaded matrices, Ch-BDGE-BBh microbeads were tested as model heterogeneous catalysts in the peroxide decomposition reaction. These microbeads were selected because of their high copper binding stability though they present a lower degree of dendronization. As shown in Fig. 5, a low decomposition percentage (8 %) was achieved for the reactions catalyzed by the control matrices Ch-BDGE, Ch-BDGE+Cu, and Ch-BDGE-BBh after 80 min. However, conversion (35 %) was reached at 50 min with Ch-BDGE-BBh+Cu. These results demonstrate the significance of a dendritic structure both in metal coordination and in catalytic activity.

Conclusions

This work combines the well-known advantages of chitosan with the multifunctionality imparted by the dendronization process, highlighting the cooperative effect conferred by dendritic structures on chitosan. A hydrophilic–hydrophobic balance was found throughout the dendronized surface, the properties changing in accordance with the size of the dendron and the number and type of functional group in the periphery.

The highest level of copper immobilization was obtained for chitosan modified with BB though the degree of dendronization with BB was lower than that with BA. The presence of the dendron also plays a major role in interacting with copper ion.

The catalytic activity of the dendronized bead was also evaluated in an oxidation reaction. A high conversion was attained for the Cu^{2+}-coordinated BB-dendronized chitosan microbeads. The results described in this paper suggest a multivalent effect due to the proximity and nature of periphery groups. In terms of pre-organization, the presence of dendrons could result in more organized molecular arrangements, thereby enhancing the efficiency of encapsulation of the metal ion. In catalysis, the relevance of organized molecular arrangements lies in their ability to influence the selectivity of the catalytic process.

The proven cooperative effect of dendronized surfaces and their effectiveness in catalytic processes form the basis for further research in this field. Steps in this direction are already being pursued.

Experimental

Materials

The following chemicals were purchased: epichlorohydrin (ECH; Riedel-de Häen), butylene diglycidyl ether (BDGE; Sigma-Aldrich), sodium carbonate (Cicarelli), tris[(*tert*-butoxycarbonyl)ethyl]aminomethane (so called Behera's amine, BA; Frontier Scientific), thionyl chloride (Merck), 5-nitroisophtalic acid (99 %, Anedra), palladium (10 wt-% on activated carbon, Pd/C Aldrich), silica gel 60 (Merck), potassium bromide (99 % FT-IR grade, Aldrich), chloroform-d (99.8 % D, Aldrich), chitosan (Ch, 85 % degree of deacetylation, low molecular weight, Aldrich), pentahydrate copper sulfate (Aldrich), phosphate buffer solution (0.5 M, Aldrich), hydrogen peroxide (98 %, Aldrich), potassium permanganate (Aldrich), sodium oxalate (Aldrich), nitric acid and hydrochloric acid (Sintorgan). Solvents were obtained from Sintorgan, purified by distillation, and dried. *N*,*N*′-bis[tris((*tert*-butoxycarbonyl)ethyl) methyl]-5-aminephtalamide (so called bis Behera's amine, BB) was prepared as previously reported.[37]

Physico-Chemical Characterization

FT-IR spectra were obtained on a Nicolet Avatar 360 FT-IR spectrometer. A Thermo Scientific Smart Diffuse Reflectance accessory was used to obtain diffuse-reflectance IR spectra. SiC discs were used to abrade the surface of different samples. All spectra were obtained with 32 scans at a 4.0 cm^{-1} resolution in a range between 4000 and 650 cm^{-1}. ^1H NMR spectra were recorded on a Brüker 400 MHz NMR spectrometer using $CDCl_3$ as solvent. SEM images of the microspheres were obtained on a Philips 501B scanning electron microscope, operating at 12 kV, at the National Institute of Industrial Technology (INTI) (Córdoba, Argentina) to analyze the microsphere morphology. DSC measurements were taken using a V5.4A from TA Instruments on samples using a mass of

~2 mg, a heating rate of 10°C min^{-1}, and testing temperatures ranging from 50 to 400°C. TGA measurements were conducted using a 2950 TGA HR V5.4A from TA Instruments on samples using a mass of ~5 mg, a heating rate of 10°C min^{-1}, nitrogen atmosphere, and testing temperatures ranging from 40 to 400°C. The dried samples were gold-coated. The copper concentration was measured on a PerkinElmer AAnalyst 100 atomic absorption spectrophotometer using a wavelength of 324.8 nm and slit width of 0.7 (APHA, 2005). Duplicate measurements were made such that the residual concentration values could be reproduced within ±2 %.

Preparation of Chitosan Microbeads

Chitosan microbeads were prepared by dissolution of polymer (1.000 g) in a 5 % (v/v) acetic acid solution (35 mL). Chitosan solution was then added dropwise into a precipitation bath containing 0.5 M NaOH solution (500 mL). This step neutralized the acetic acid within the chitosan gel, thus coagulating the gel into uniformly spherical chitosan gel beads. A magnetic stirrer was used to stir the aqueous NaOH solution continuously at 200 rpm to prevent the beads from sticking to one another or to the glassware surface. The wet chitosan beads were filtered and extensively rinsed with distilled water to remove NaOH. They were then air-dried to eliminate water and subsequently modified with ECH or BDGE according to the following procedure.

The Ch-ECH and Ch-BDGE microbeads were prepared as follows. The chitosan microbeads (0.5000 g) were added to a 0.1 M spacer (ECH or BDGE) solution (30 mL) to obtain a 1 : 1 ratio with chitosan (mol spacer: mol OH group of chitosan). The solutions were heated to 45°C for 2 h and stirred continuously using a magnetic stirrer at 200 rpm. The beads were then filtered, washed with distilled water to remove excess ECH or BDGE solution, and air-dried. The oxirane groups were determined by the pyridinium chloride method.[38]

Dendronization of Ch-ECH and Ch-BDGE Microbeads

Ch-ECH and Ch-BDGE microbeads were soaked in water (100 mg mL^{-1}) for 24 h. BA and BB (4.50 mg and 10.7 mg, respectively), dissolved in 0.2 M Na_2CO_3 (0.08 mL), were then added to the swollen microbeads and stirred at 60°C for 36 h. The mol ratio corresponding to the epoxy/dendron was 1 : 0.6, which is optimal for dendron coupling because the addition of dendron does not increase the degree of dendronization. Ch-ECH-BA, Ch-ECH-BB, Ch-BDGE-BA, and Ch-BDGE-BB were filtered and washed with water, 0.1 N acetic acid solution, and water again. The products were then dried and the amount of linked dendrons was determined via oxirane group determination using the pyridinium chloride method.[38]

Hydrolysis of t-Butyl Groups of Dendritic (BA and BB) Periphery

Hydrolysis of the ester groups on the dendritic surface was carried out in 85 % v/v formic acid at 60°C for 4 days, after which the microbeads were washed, dried, and labelled as Ch-ECH-BAh, Ch-ECH-BBh, Ch-BDGE-BAh, and Ch-BDGE-BBh. The degree of hydrolysis was determined by the acid–base titration.

Copper Retention and Desorption

The modified microbeads (10.0 mg) were placed in 25 ppm $CuSO_4$ solution (3.0 mL) at pH 5 for 4 days. The solution was then filtered and the copper ion in solution was determined by atomic spectroscopy, thereby enabling the copper ion retention to be calculated. For the desorption experiment, the microbeads (10.0 mg) were brought into contact with 1 M HNO_3 solution (2.0 mL) for 24 h. The solution was then filtered and the copper ion in solution was determined by atomic spectroscopy. Finally, the recovered values of the copper ion were calculated.

Hydrogen Peroxide Catalysis

A flask containing a mixture of hydrogen peroxide ($c_0 = 5$ mM) and the studied catalyst (1.4 g L^{-1}) was shaken during reaction to provide sufficient dispersion of the catalyst particles. The reaction was placed in 5 mM phosphate buffer solution under standard atmospheric conditions. Samples of solution taken at various points in time were filtered, and the hydrogen peroxide concentration was measured by the permanganate titration method.

Swelling Studies

The water sorption capacity of the chitosan microbeads was determined by swelling in buffer of pHs 1.2 and 7.4 at room temperature. The known weight of each microbead sample was placed in the medium until equilibrium swelling was attained. The percentage swelling (E_{sw}) in the medium was calculated using Eqn 2:

$$E_{sw}(\%) = \frac{W_s - W_o}{W_o} \times 100\,\%$$

where W_s denotes the weight of the chitosan microbeads at equilibrium swelling and W_o the initial weight of the microbeads. Each swelling experiment was repeated twice and the average value was taken as the E_{sw} value.

Supplementary Material

Figures showing the synthetic route of the dendronized microbeads (Fig. S1); structures of the dendronized chitosan microbeads (Fig. S2); FT-IR spectrum of BA (Fig. S3) and the diffuse-reflectance FT-IR spectra of Ch-BDGE-BB and copper-sorbed Ch-BDGE-BB; 1H-NMR spectra of BA (b-1) and BA-Cu (b-2) (Fig. S4a, b) are available on the Journal's website.

Acknowledgements

The authors gratefully acknowledge financial assistance from Fund for Scientific and Technological Research (FONCYT), National Council of Scientific and Technical Research (CONICET), and Secretary of Science and Technology of National University of Córdoba (SECYT-UNC). A.A.A. thanks CONICET for the fellowship awarded. We thank Gloria Bonetto of the NMR Laboratory of the Faculty of Chemical Science (National University of Córdoba) for recording the spectra and Prof. Dr Marcelo Calderón (Freie Universität Berlin) for assistance in the preparation of this manuscript.

References

[1] O. G. da Silva, M. G. da Fonseca, L. N. H. Arakaki, *Colloids Surf., A* **2007**, *301*, 376. doi:10.1016/J.COLSURFA.2006.12.072

[2] J. I. Paez, M. Martinelli, V. Brunetti, M. C. Strumia, *Polymers (Basel, Switz.)* **2012**, *4*, 355. doi:10.3390/POLYM4010355

[3] R. S. Bagul, N. Jayaraman, *J. Organomet. Chem.* **2012**, *701*, 27. doi:10.1016/J.JORGANCHEM.2011.11.026

[4] R. T. Lee, H.-J. Gabius, Y. C. Lee, *Carbohydr. Res.* **1994**, *254*, 269. doi:10.1016/0008-6215(94)84259-0

[5] M. Kröger, O. Peleg, A. Halperin, *Macromolecules* **2010**, *43*, 6213. doi:10.1021/MA100861B
[6] O. Iliashevsky, L. Amir, R. Glaser, R. S. Marks, N. G. Lemcoff, *J. Mater. Chem.* **2009**, *19*, 6616. doi:10.1039/B908014G
[7] J. I. Paez, M. C. Strumia, M. C. G. Passeggi, Jr, J. Ferrón, A. M. Baruzzi, V. Brunetti, *Electrochim. Acta* **2009**, *54*, 4192. doi:10.1016/J.ELECTACTA.2009.02.064
[8] M. Rinaudo, *Prog. Polym. Sci.* **2006**, *31*, 603. doi:10.1016/J.PROGPOLYMSCI.2006.06.001
[9] M. Monier, A. El-Mekabaty, *Int. J. Biol. Macromol.* **2013**, *55*, 207. doi:10.1016/J.IJBIOMAC.2013.01.020
[10] M. Pau Balaguer, R. Gavara, P. Hernández-Muñoz, *Food Chem.* **2012**, *130*, 814. doi:10.1016/J.FOODCHEM.2011.07.052
[11] S.-L. Wang, T.-W. Liang, Y.-H. Yen, *Carbohydr. Polym.* **2011**, *84*, 732. doi:10.1016/J.CARBPOL.2010.06.022
[12] V. K. Thakur, M. K. Thakur, P. Raghavan, M. R. Kessler, *ACS Sustainable Chem. Eng.* **2014**, *2*, 1072. doi:10.1021/SC500087Z
[13] V. K. Thakur, M. K. Thakur, R. K. Gupta, *Int. J. Poly. Anal. Charact.* **2014**, *19*, 256. doi:10.1080/1023666X.2014.880016
[14] V. K. Thakur, M. K. Thakur, R. K. Gupta, *Carbohydr. Polym.* **2013**, *98*, 820. doi:10.1016/J.CARBPOL.2013.06.072
[15] V. K. Thakur, M. K. Thakur, R. K. Gupta, *Carbohydr. Polym.* **2013**, *97*, 18. doi:10.1016/J.CARBPOL.2013.04.069
[16] V. K. Thakur, M. K. Thakur, *ACS Sustainable Chem. Eng.* **2014**, *2*, 2637. doi:10.1021/SC500634P
[17] V. K. Thakur, M. K. Thakur, *Carbohydr. Polym.* **2014**, *109*, 102. doi:10.1016/J.CARBPOL.2014.03.039
[18] V. K. Thakur, M. K. Thakur, R. K. Gupta, *Int. J. Biol. Macromol.* **2013**, *61*, 121. doi:10.1016/J.IJBIOMAC.2013.06.045
[19] V. K. Thakur, M. K. Thakur, R. K. Gupta, *Int. J. Biol. Macromol.* **2013**, *62*, 44. doi:10.1016/J.IJBIOMAC.2013.08.026
[20] A. A. Aldana, R. Toselli, M. C. Strumia, M. Martinelli, *J. Mater. Chem.* **2012**, *22*, 22670. doi:10.1039/C2JM33100D
[21] G. L. Rorrer, T. Y. Hsien, J. D. Way, *Ind. Eng. Chem. Res.* **1993**, *32*, 2170. doi:10.1021/IE00021A042
[22] F.-L. Mi, H.-W. Sung, S.-S. Shyu, *J. Polym. Sci., Part A: Polym. Chem.* **2000**, *38*, 2804. doi:10.1002/1099-0518(20000801)38:15<2804::AID-POLA210>3.0.CO;2-Y
[23] L. Fernandez, M. Calderón, M. Martinelli, M. Strumia, H. Cerecetto, M. González, J. J. Silber, M. Santo, *J. Phys. Org. Chem.* **2008**, *21*, 1079. doi:10.1002/POC.1448
[24] L. G. Wade, in *Organic Chemistry* (Ed. A. Jaworski) **2013**, Ch. 19, pp. 439–466 (Pearson: London).
[25] D. E. S. Santos, C. G. T. Neto, J. L. C. Fonseca, M. R. Pereira, *J. Membr. Sci.* **2008**, *325*, 362. doi:10.1016/J.MEMSCI.2008.07.050
[26] A. A. Aldana, M. C. Strumia, M. Martinelli, *J. Biomater. Tissue Eng.* **2013**, *3*, 157. doi:10.1166/JBT.2013.1075
[27] R. Laus, T. G. Costa, B. Szpoganicz, V. T. Fávere, *J. Hazard. Mater.* **2010**, *183*, 233. doi:10.1016/J.JHAZMAT.2010.07.016
[28] C. K. S. Pillai, W. Paul, C. P. Sharma, *Prog. Polym. Sci.* **2009**, *34*, 641. doi:10.1016/J.PROGPOLYMSCI.2009.04.001
[29] M. Eichler, V. Katzur, L. Scheideler, M. Haupt, J. Geis-Gerstorfer, G. Schmalz, S. Ruhl, R. Müller, F. Rupp, *Biomaterials* **2011**, *32*, 9168. doi:10.1016/J.BIOMATERIALS.2011.08.063
[30] F. Xi, J. Wu, *J. Chromatogr. A* **2004**, *1057*, 41. doi:10.1016/J.CHROMA.2004.09.059
[31] S. R. Popuri, Y. Vijaya, V. M. Boddu, K. Abburi, *Bioresour. Technol.* **2009**, *100*, 194. doi:10.1016/J.BIORTECH.2008.05.041
[32] R. Šuláková, R. Hrdina, G. M. B. Soares, *Dyes Pigm.* **2007**, *73*, 19. doi:10.1016/J.DYEPIG.2005.10.004
[33] U. Boas, P. M. H. Heegaard, *Chem. Soc. Rev.* **2004**, *33*, 43. doi:10.1039/B309043B
[34] M. Rajiv Gandhi, G. N. Kousalya, N. Viswanathan, S. Meenakshi, *Carbohydr. Polym.* **2011**, *83*, 1082. doi:10.1016/J.CARBPOL.2010.08.079
[35] J. M. Lázaro Martínez, E. Rodríguez-Castellón, R. M. T. Sánchez, L. R. Denaday, G. Y. Buldain, V. Campo Dall' Orto, *J. Mol. Catal. Chem.* **2011**, *339*, 43. doi:10.1016/J.MOLCATA.2011.02.010
[36] M. Hermanek, R. Zboril, I. Medrik, J. Pechousek, C. Gregor, *J. Am. Chem. Soc.* **2007**, *129*, 10929. doi:10.1021/JA072918X
[37] A. A. Aldana, M. Martinelli, M. Strumia, *Macromol. Symp.* **2010**, *298*, 99. doi:10.1002/MASY.201000035
[38] H. Lee, K. Neville, *Handbook of Epoxy Resins* **1967** (McGraw-Hill: Michigan).